Derivatives of 5-Nitro-furan-2-carboxylic Acid Carbamoylmethyl Ester Inhibit RNase H Activity Associated with HIV-1 Reverse Transcriptase

Hideyoshi Fuji,[†,‡] Emiko Urano,[†,§,||] Yuko Futahashi,[||] Makiko Hamatake,[||] Junko Tatsumi,[‡] Tyuji Hoshino,[‡] Yuko Morikawa,[§] Naoki Yamamoto,[||] and Jun Komano*[,||]

Department of Physical Chemistry, Graduate School of Pharmaceutical Sciences, Chiba University, 1-33 Yayoi-cho, Inage-ku, Chiba, 263-8522, Japan, Kitasato Institute of Life Sciences, Kitasato University, Shirokane 5-9-1, Minato-ku, Tokyo, 108-8641, Japan, AIDS Research Center, National Institute of Infectious Diseases, 1-23-1 Toyama, Shinjuku, Tokyo 162-8640, Japan

Received August 28, 2008

The RNase H activity associated with human immunodeficiency virus type 1 (HIV-1) is an attractive target for an antiretroviral drug development. We screened 20000 small-molecular-weight compounds for RNase H inhibitors and identified a novel RNase H-inhibiting structure characterized by a 5-nitro-furan-2-carboxylic acid carbamoylmethyl ester (NACME) moiety. Two NACME derivatives, 5-nitro-furan-2-carboxylic acid adamantan-1-carbamoylmethyl ester (compound **1**) and 5-nitro-furan-2-carboxylic acid [[4-(4-bromo-phenyl)-thiazol-2-yl]-(tetrahydro-furan-2-ylmethyl)-carbamoyl]-methyl ester (compound **2**), effectively blocked HIV-1 and MLV RT-associated RNase H activities with IC_{50}s of 3−30 μM but had little effect on bacterial RNase H activity in vitro. Additionally, 20−25 μM compound **2** effectively inhibited HIV-1 replication. An in silico docking simulation indicated that the conserved His539 residue, and two metal ions in the RNase H catalytic center are involved in RNase H inhibition by NACME derivatives. Taken together, these data suggest that NACME derivatives may be potent lead compounds for development of a novel class of antiretroviral drugs.

Introduction

Highly Active Anti-Retroviral Therapy, a combination of antiretroviral drugs, has become the standard treatment for HIV-infected individuals. However, the emergence of drug-resistant viruses is problematic because there are few alternative treatment regimens. HIV-1[a] has three known enzymes, protease, reverse transcriptase (RT), and integrase (IN). The RT, a heterodimer of p51 and p66 subunits, has three enzymatic functions: RNA- and DNA-dependent DNA polymerase and RNase H activity. Inhibitors of the protease, RT-associated polymerase, and IN activities are now in clinical use; however, a suitable inhibitor of the RT-associated RNase H activity has not been found. Thus, developing a highly specific inhibitor against HIV-1 RT-associated RNase H activity could provide another option for treatment of HIV-1-infected individuals.

RNase H activity is a ribonuclease activity that recognizes RNA hybridized to DNA. The RT-associated RNase H activity resides in the carboxy-terminal region of p66 and is essential for synthesis of double-stranded DNA from the HIV-1 single-stranded RNA genome. The RNase H activity is also involved in HIV-1 drug resistance to RT inhibitors as well as generating a diversity of viruses in vivo by homologous recombination.[1−7] Thus, RT-associated RNase H activity is another attractive target for development of a novel class of antiretroviral drugs.[8] Dual inhibitors that target RNase H and IN or RT-associated polymerase activities have been reported because these enzymes possess structural similarities.[9−11] Such inhibitors should be more effective than inhibitors that merely target RNase H activity.

The difficulty in developing an RNase H inhibitor for the treatment of HIV-1 infection lies in the specificity and toxicity of the drug. Although several RNase H inhibitors with different structures have been reported,[9,12−20] the 50% inhibitory concentration (IC_{50}) of many previous derivatives are on the order of micromolar concentration and they often lack sufficient specificity for the HIV-1 RT-associated RNase H activity. Most problematically, they often display cytotoxicity to mammalian cells. Many RNase H inhibitors are assumed to bind to the catalytic center and interact with Mg^{2+} ions. The toxicity of such inhibitors may be due to inhibition of other cellular proteins that require divalent metal cations to function.

More chemical compounds need to be tested in order to find a novel RNase H inhibitor with a chemical structure that can be used to design a potent and specific HIV-1 RNase H inhibitor. For a structure−function based approach to drug design, the chemical−enzyme interactions are examined by in silico docking simulations and the models critically assessed by comparing them to data obtained from experiments. This approach is possible because the crystallized protein structures of the HIV-1 RT and RNase H proteins from diverse organisms have been solved. Indeed, structure-based drug design has been successful in identifying several of the drugs currently available for HIV-1 treatment including protease inhibitors. Molecular docking simulations can reveal the molecular details of the interaction between HIV-1 RT and RNase H inhibitors.

In this study, we screened 20000 small molecular weight compounds to find chemicals that suppress the HIV-1 RT-associated RNase H activity. We found that derivatives of 5-nitro-furan-2-carboxylic acid carbamoylmethyl ester inhibit retroviral RNase H activity in vitro. One of the derivatives was

* To whom correspondence should be addressed. Phone: +81-3-5285-1111. Fax: +81-3-5285-5037. E-mail: ajkomano@nih.go.jp.

† These authors equally contributed to this work.

‡ Department of Physical Chemistry, Graduate School of Pharmaceutical Sciences, Chiba University.

§ Kitasato Institute of Life Sciences, Kitasato University.

|| AIDS Research Center, National Institute of Infectious Diseases.

[a] Abbreviations: HIV-1, human immunodeficiency virus type 1; RT, reverse transcriptase; NACME, 5-nitro-furan-2-carboxylic acid carbamoylmethyl ester; compound 1, 5-nitro-furan-2-carboxylic acid adamantan-1-carbamoylmethyl ester; compound 2, 5-nitro-furan-2-carboxylic acid [[4-(4-bromo-phenyl)-thiazol-2-yl]-(tetrahydro-furan-2-ylmethyl)-carbamoyl]-methyl ester.

10.1021/jm801071m CCC: $40.75
Published on Web 01/29/2009

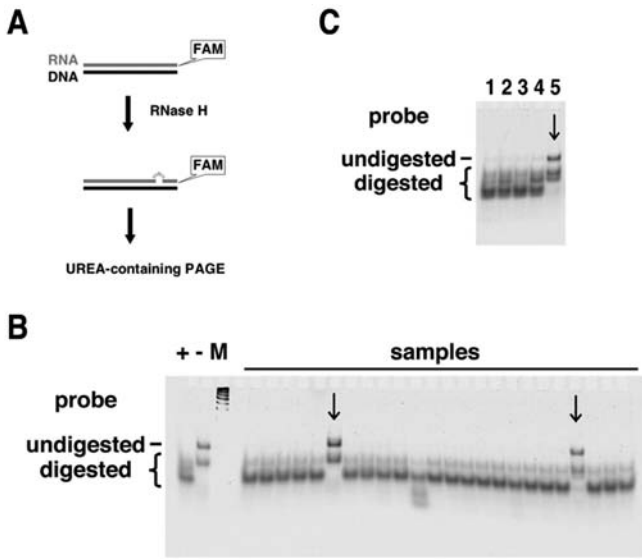

Figure 1. Screening for RNase H inhibitors. (A) Schematic diagram of the screening method. (B) An example from the first screen. Groups of 5 chemicals were pooled at 100 μM each for testing. Some pools exhibited RNase H inhibitory activity (arrows). (C) An example from the second screen. The five chemicals from a positive pool were tested individually at 100 μM each. One of the chemicals was responsible for the RNase H inhibition (arrow).

able to limit HIV-1 replication in tissue culture. The docking simulations were consistent with the experimental data and indicate some critical drug−enzyme interactions. The in silico docking simulation may help us to design a highly specific inhibitor against HIV-1 RT-associated RNase H activity.

Results

To find a novel chemical that inhibits HIV-1 RT-associated RNase H activity, we screened a chemical library containing 20000 compounds representing key structural features of three million chemicals. We used a purified RT encoded by a clade B HIV-1_{LAI} and a polyacrylamide gel electrophoresis (PAGE)-based assay for the first and second rounds of screening (Figure 1A). A fluorochrome-labeled synthetic oligoribonucleotide was annealed to a complementary oligodeoxyribonucleodide, and the hybridized DNA/RNA probe was incubated with HIV-1 RT. The RT-associated RNase H activity introduces nicks into the RNA strand that yields low molecular weight bands in UREA-containing denaturing PAGE, which are visualized by fluorescence scanning. The p51 preparation did not yield detectable low-molecular-weight bands, indicating that the RT preparation was not contaminated with RNase activities of bacterial origin (data not shown). Initially, five chemicals were pooled for screening purposes, and the screen was performed with each chemical at a concentration of 100 μM. Some of the pooled chemicals protected the RNA/DNA probe from cleavage by the RT-associated RNase H (Figure 1B). Pooled chemicals that showed ~50% protection efficiency were chosen for the second round of screening (43/20000 chemicals, 0.22%). Individual chemicals were tested at a concentration of 100 μM (Figure 1C). We found 17 chemicals (0.085%) that possessed detectable RNase H inhibitory activities. Interestingly, six of these compounds (6/17 chemicals, 35.3%) included a common structure characterized by a 5-nitro-furan-2-carboxylic acid carbamoylmethyl ester (NACME, Figure 2A).

To clarify the structure−activity relationship, we re-examined 91 chemicals from the chemical library bearing NACME homologues and tested their RNase H inhibitory activity using a real-time monitoring assay described previously.[21] Among these 91 chemicals, 32 compounds displayed detectable RNase H inhibition (32/91 chemicals, 35.2%). Derivatives carrying various substituents at the end of the carbamoylmethyl ester group (R1) retained RNase H inhibitory activity (32/48 chemicals, 66.7%; Figure 2A,B), but substitution of the 5-nitro-furan (R2) with various structures resulted in a loss of RNase H inhibition. These data indicate a critical role for the 5-nitro-furan group in RNase H inhibition (0/43 chemicals, 0.0%; Figure 2C). NACME derivatives displayed RNase H inhibitory activity when R1 was substituted by a relatively long and bulky group (Figure 2A). Conversely, compounds with relatively small volume substituents in the R1 position showed no inhibitory activity (Figure 2B). A steric effect could explain why some derivatives with large substituents that did not show RNase H inhibitory activity (Figure 2A,B). We tested a series of additional NACME derivatives not included in the original chemical library and found that five compounds inhibited RNase H (5/20 chemicals, 20%). The significant increase in the percentage of RNase H inhibitors in this "biased" population compared to the original library (20.0% vs 0.085%, 235.3-fold) suggests that the NACME motif is a novel RNase H inhibitory structure. We focused on two representative derivatives for detailed analysis: 5-nitro-furan-2-carboxylic acid adamantan-1-carbamoylmethyl ester (compound **1**, hereafter) and 5-nitro-furan-2-carboxylic acid [[4-(4-bromo-phenyl)-thiazol-2-yl]-(tetrahydro-furan-2-yl-methyl)-carbamoyl]-methyl ester (compound **2**, hereafter; Figure 2A).

The IC_{50}s of compounds **1** and **2** for the HIV-1 RT-associated RNase H were defined as the concentration of the chemical yielding half the substrate cleavage rate of the control (DMSO) and were measured using the real time monitoring assay[21] (Figure 3A). The estimated IC_{50}s for compounds **1** and **2** for clade B HIV-1_{LAI}-derived RT-associated RNase H activity were 29.6 ± 9.2 μM (n = 6) and 26.7 ± 13.5 (n = 5), respectively (Figure 3B and Table 1). Similar IC_{50}s were obtained in assays performed independently by Beutler et al. (data not shown) with a previously described protocol.[22] RTs from different HIV-1 strains were also tested. The IC_{50}s of compounds **1** and **2** for the HIV-1 clade C (93IN101) RT were 26.5 ± 15.0 μM (n = 5) and 32.2 ± 7.5 μM (n = 3) and for the CRF01 A_E (93JP-NH1) RT were 3.8 ± 1.5 μM (n = 3) and 2.6 ± 1.8 μM (n = 5), respectively (data not shown, Figure 3B, and Table 1). The IC_{50}s of compounds **1** and **2** for a murine leukemia virus (MLV) RT were 8.4 ± 9.4 μM (n = 6) and 8.6 ± 8.9 μM (n = 7), respectively (Figure 3B and Table 1). Neither compound inhibited RNase H from *Escherichia coli* (data not shown). Of note, inhibitory activity against human RNase H1 was observed for compound **2** (IC_{50} ~50 μM) but not compound **1** (Beutler et al., data not shown). The enzymatic activities of the HIV-1 IN and the RT RNA-dependent DNA polymerase were not detectably affected by these compounds (data not shown, Pommier et al., data not shown; Table 1). These data suggest that compounds **1** and **2** specifically inhibit RNase H.

We examined whether these compounds were able to limit HIV-1 replication using two assay systems. The 50% cytotoxicity concentration was >25 μM for T cell lines and NP2CD4-CXCR4 cells, and 25−50 μM for primary $CD4^+$ T cells (data not shown). First, we infected NP2CD4CXCR4 cells with HIV-1_{NL4-3} in the presence of compound **2**. Four days postinfection, the culture supernatant was recovered and the concentration of viral p24 antigen was measured by ELISA. The p24 levels decreased in an compound 2 dose-dependent manner, and the

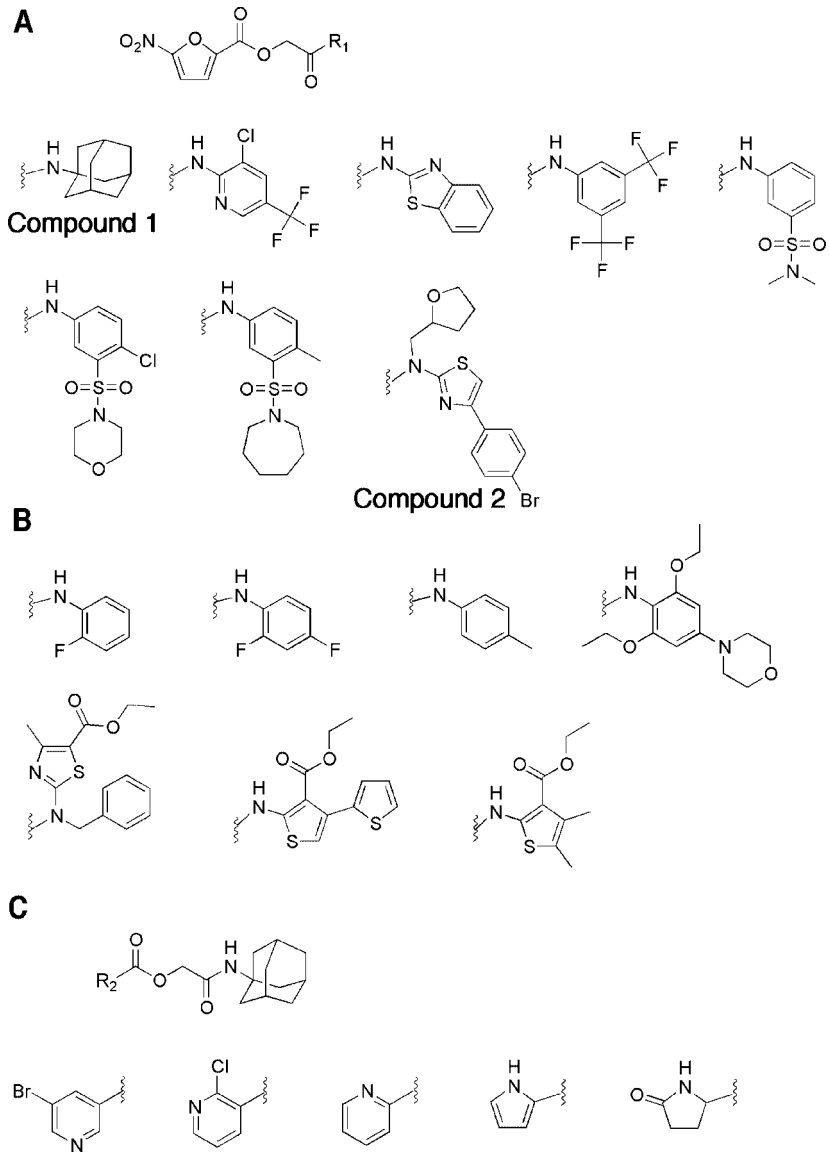

Figure 2. Structure−activity relationships of NACME homologues. (A) NACME derivatives with RNase H inhibitory activity carrying various substituents at the R1 position. The structure at the top is the NACME core structure. The structures below are the R1 substituents. (B) NACME derivatives with no RNase H inhibitory activity carrying various substituents at the R1 position. The structures show the R1 substituents. (C) NACME derivatives carrying various chemical structures at the R2 position. None of these chemicals displayed RNase H inhibitory activity.

IC_{50} was estimated to be ~22.7 μM (Figure 4A). Finally, we infected primary $CD4^+$ T cells with HIV-1_{NL4-3} and monitored the viral replication kinetics in the presence of 25 μM compounds **1** or **2**. Compared to control, HIV-1_{NL4-3} replication was slowed to some extent by compound **1**, but a greater attenuation of viral replication was observed in the presence of compound **2** (Figure 4B).

We conducted an in silico docking simulation using the GOLD software and the RT structure of PDB code: 1RTD[23] to examine the molecular mechanism of RNase H inhibition. Overall docking results for compounds **1** and **2** were similar (Figure 5A−C). The best docking pose for compound **1** showed that the nitrofuran group chelates the two Mg^{2+} ions and orients toward His539 to form a possible hydrogen bond (Figure 5B). Additionally, the carbonyl oxygen atom in the amide group of compound **1** interacted with the side chain of Ser553. There were hydrophobic contacts between the adamantan group of compound **1** and the side chain of Lys550. For compound **2**, the best docking pose showed that, in addition to the above interactions, a nitrogen atom in the thiazole group interacted with Asp549 by hydrogen bonding (Figure 5C). A hydrophobic contact between the phenyl group of compound **2** and the side chain of Glu546 was also observed (Figure 5C). In contrast, most of the inactive compounds did not chelate the two Mg^{2+} ions simultaneously, and His539 was not involved in the chemical−enzyme interaction (Figure 5D). The possible interactions of compounds **1** and **2** with the RNase H domain of HIV-1 RT are summarized in Figure 5E. Similar findings were obtained by additional simulation using the Glide (Schrodinger Inc.) docking simulation software (data not shown). These results suggest that the interactions with both of the Mg^{2+} ions and His539 are essential to the inhibition of HIV-1 RNase H activity by NACME derivatives. We measured the ChemScores of compounds **1** and **2** in binding to HIV-1 RT and compared the scores with those of the *E. coli* and human RNase H using X-ray structures of *E. coli* (PDB code: 1RDD[24]) and human RNase H (RNase H1, PDB code: 2QKK[25]). For compound **2**, the ChemScores were 31.27, 18.02, and 26.03 against HIV-1, *E. coli*, and human RNase H, respectively. For compound **1**, the ChemScores were 30.79, 17.09, and 28.10, respectively. In

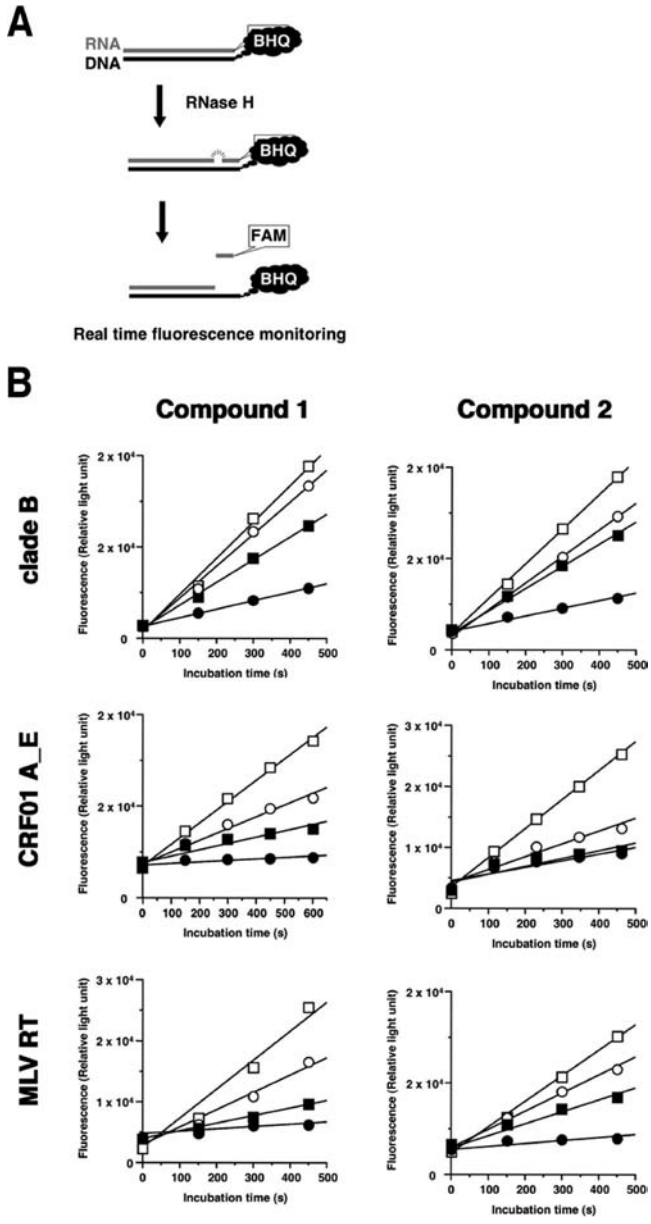

Figure 3. Measuring the IC_{50}s of compounds **1** and **2** against various RNase H activities. (A) Schematic presentation of the experimental system. The black hole quencher (BHQ) blocks the fluorescence emission from FAM when placed close to FAM. (B) Real-time monitoring of RNase H activity in the presence of increasing concentrations of compounds **1** (left) and **2** (right). HIV-1 RT derived from clade B and CRF01 A_E, and MLV RT were tested (top to bottom, respectively). Drug concentrations were 50 (solid circle), 10 (solid square), 2 (open circle), and 0 μM (DMSO, open square), respectively.

Table 1. Summary of Compounds **1** and **2** IC_{50}s

enzyme	compd **1**	compd **2**
HIV-1 RT		
clade B, μM	29.6 ± 9.2 (n = 6)	26.7 ± 13.5 (n = 5)
clade C, μM	26.5 ± 15.0 (n = 5)	32.2 ± 7.5 (n = 3)
CRF01 A_E, μM	3.8 ± 1.5 (n = 3)	2.6 ± 1.8 (n = 5)
MLV RT, μM	8.4 ± 9.4 (n = 6)	8.6 ± 8.9 (n = 7)
E. coli RNase H	no inhibition	no inhibition
human RNase H1, μM	no inhibition	~50
HIV-1 IN	no inhibition	no inhibition

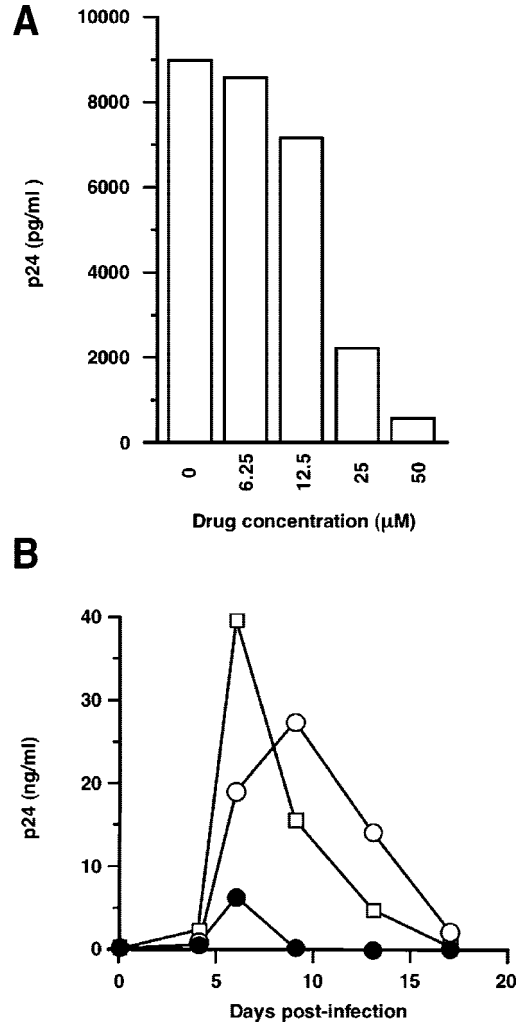

Figure 4. Inhibition of HIV-1 replication by compounds **1** and **2**. (A) Inhibition of HIV-1 replication by compound **2** was measured using the NP2CD4CXCR4/ HIV-1_{NL4-3} system. The estimated IC_{50} was ~22.7 μM. (B) Effect of compound **1** (open circle) and compound **2** (filled circle) on HIV-1_{NL4-3} replication in PBMC. DMSO was used for the negative control (square).

agreement with the in vitro experiments, the ChemScores against *E. coli* RNase H were the lowest for both inhibitors. Inhibition of human RNase H by compound **2** can be explained by the docking structure, which indicated that compound **2** interacted with the highly conserved His264 (which corresponds to the HIV-1 His539) and two metal ions simultaneously in the human RNase H active site. In contrast, there is no interaction between compound **1** and His264 in the human RNase H. Similarly, there was no interaction between either inhibitor and the highly conserved His124 (which corresponds to the HIV-1 His539) of the *E. coli* RNase H. These data justify the reliability of docking simulation results and suggest a critical role of the conserved His residues in regulating RNase H function.

Discussion

This is the first report characterizing the NACME moiety as a functional group with the ability to inhibit HIV-1 RT-associated RNase H activity. The representative NACME derivatives compounds **1** and **2** were able to inhibit RTs derived from various HIV-1 clades with varying potencies. However, compounds **1** and **2** did not inhibit IN or RT polymerase activities, indicating that NACME derivatives are specific RNase H inhibitors.

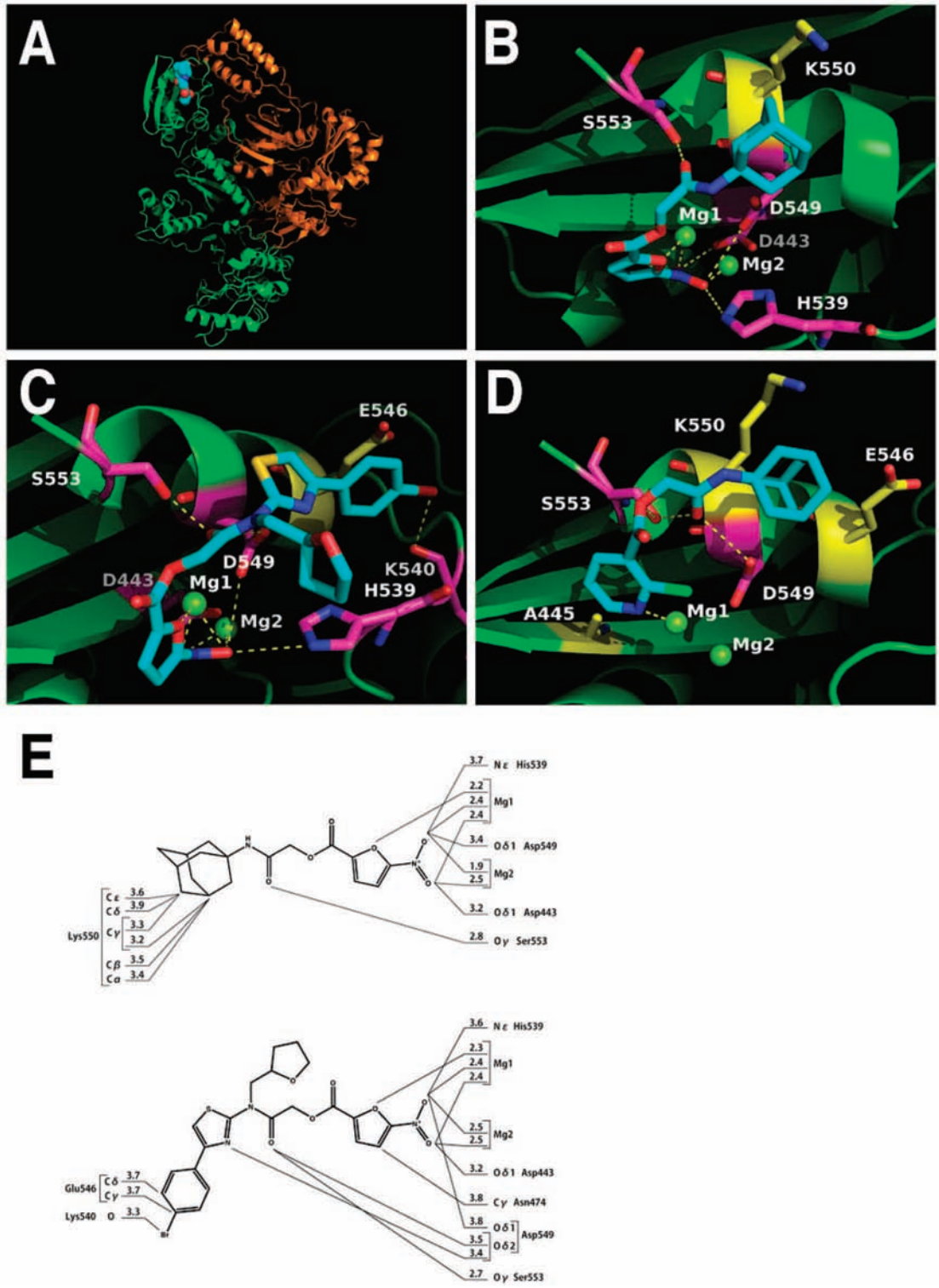

Figure 5. In silico simulation of compounds **1** or **2** docking to the RNase H domain of HIV-1 RT. (A) Overview of HIV-1 RT docked with compound **1**. HIV-1 RT is depicted as a ribbon model, with p66 in green and p51 in orange. Compound **1** is shown using a space filling model with carbon in cyan, oxygen in red, and nitrogen in blue. (B) Structure of compound **1** bound to the RNase H domain. (C) Structure of compound **2** bound to the RNase H domain. (D) Structure of a noninhibitor bound to the RNase H domain. NACME derivatives are presented as stick model with carbon in cyan, oxygen in red, nitrogen in blue, sulfur in yellow, bromine in brown, and chlorine in green. HIV-1 RNase H is depicted in a ribbon mode in green. Magnesium ions are depicted as green sheres. Amino acid residues forming hydrophobic contacts with NACME derivatives are depicted by yellow stick models. Amino acid residues forming hydrogen bonds with compounds **1** or **2** are depicted by magenta stick models, and hydrogen bonds are in dashed yellow lines. Figures were generated by PyMOL. (E) Atoms of compound **1** (top) and compound **2** (bottom) that may interact with amino acids and Mg^{2+} ion in HIV-1 RT are shown with contact distances. All residues in contact with the compounds are from the RNase H domain of HIV-1 RT.

It is intriguing that HIV-1 replication was restricted by compound **2** because most RNase H inhibitors are unable to inhibit HIV-1 replication in tissue culture. RDS1643 is one of the diketo RNase H inhibitors and has been shown to inhibit HIV-1 replication in vivo at micromolar concentrations.[12] Although we detected the anti-HIV-1 activity of compound **2**,

the cytotoxicity still remained a concern because the selectivity window was small. Compound **2** and RDS1643 still need to be improved to lower both IC_{50} and the cytotoxicity. Compound **1** did not show a strong anti-HIV-1 replication activity in tissue culture even though the IC_{50}s of compounds **1** and **2** were similar in vitro. NACME is composed of many polar chemical groups; thus, NACME derivatives may have difficulty crossing a lipid bilayer. Cell membrane permeability may be conferred by the hydrophobic groups compound **2**, so that the intracellular concentration of compound **2** can reach higher levels than compound **1**. Alternatively, compound **1** may be less stable in vivo than compound **2** or cellular enzymes may attack the ester group to degrade compound **1**, whereas compound **2** may be protected sterically. As the docking model indicates, compound **2** has more contacts in the protein−drug complex than compound **1**, suggesting that the binding of compound **2** to HIV-1 RNase H may be more specific and stable than that of compound **1** in vivo. Therefore, further modifications should be considered to lower the IC_{50} of NACME derivatives to inhibit HIV-1 replication and achieve specificity.

The feasibility of the drug−protein docking structure was supported by the following evidence: two independent simulation softwares programs (GOLD and Glide) gave similar drug−protein interaction models, the predicted binding affinities from the simulations were largely consistent with the experimental data as demonstrated by the inverse correlation between docking scores and IC_{50}s, and the involvement of conserved His residues and metal ions in the predicted drug−enzyme interactions at the RNase H catalytic center. The human RNase H1 was weakly inhibited by compound **2** but not with compound **1**, where the ChemScore of compound **1** was slightly higher than that of compound **2**. This could be explained by compound **1**'s hydrophobic interaction with Met212 and Phe213 of human RNase H1 that compound **2** lacks, which may result in lowering the compound **1**'s ability to inhibit human RNase H1 activity. It is also possible that the modest ChemScore difference between compounds **1** and **2** may be within the cross validation error.[26] Compounds **1** and **2** are predicted to interact with both Asp443 and Asp549, chelators of magnesium ion. On the other hand, the inactive NACME compounds depicted in Figure 5D are predicted to interact only with D549 but not with D443. Thus, we propose a hypothesis that the interaction of NACME compounds to both D443 and D549 is important for their abilities to inhibit RNase H activity. The metal ions are essential for RNase H function[27] and His539, highly conserved residue, plays an important role in binding the scissile phosphate of the RNA.[28] Results from previous studies have shown that mutation of His539 in RT leads to a significant reduction in RNase H activity.[29] The three-dimensional structure of the RNase H domain is similar among HIV-1, *E. coli*, and human enzymes. In the catalytic center, several conserved amino acids can be identified including the His residue: His539 of HIV-1 RT, His124 of *E. coli* RNase H, and His264 of Human RNase H1. The presence of predicted contacts between compounds **1** or **2** and His539 correlated well with their ability to inhibit RNase H activity. On the basis of the structural models, we hypothesize that compounds **1** and **2** block RNase H activity by interfering with the role of His539 and the metal ions rather than through the physical interference with nucleic acid−enzyme binding because RT has sufficient molecular surface available for nucleic acid binding.

Compounds **1** and **2** showed lower IC_{50}s against RNase H from the HIV-1 clade CRF01 A_E compared to those against HIV-1 clade B and C, even when using enzymes with comparable purities and RT polymerase activities. The amino acids at or close to the RNase H active site are identical among the clade B, C, and CRF01 A_E enzymes. The subtle amino acid changes present at noncatalytic site regions could affect enzyme function. For HIV-1 RT, mutations in the connection or RNase H domains, remote from the polymerase catalytic site, were shown to affect the polymerase function.[30−32] The nonnucleoside RT inhibitor efavirenz positively affects the RNase H activity even though the binding site is distinct from the RNase H catalytic site.[33] Thus, we hypothesize that the structure of the RNase H domain of clade A_E RT is affected by noncatalytic site amino acids that differ from the clade B or C RT in such a way that compounds **1** and **2** can access and/or bind to the RNase H catalytic site more efficiently (Figure S1, Supporting Information). It is also possible that the altered RNase H structure may allow NACME derivatives to bind more tightly by generating additional drug−protein interactions.

Cytotoxicity was not detected for compound **1** but was detected for compound **2** at concentrations of 30 μM or more depending upon the cell line. Despite the differences in primary structure between HIV-1 RNase H and human RNase H, their three-dimensional structures are remarkably similar. The specificity to HIV-1 RNase H needs to be improved based on in silico design, to decrease the binding affinity between NACME derivatives and human RNase H, and thereby decrease the cytotoxicity of these inhibitors.

To improve the efficacy of NACME derivatives, we propose to attach additional chemical moieties at the carbamoyl ester side to fill pockets connected to the active site of the enzyme. Replacing polar atoms with less polar atoms should be considered to increase the hydrophobicity and allows the compound to cross the plasma membrane. A cell permeant chemical could be taken orally. Also, the ester group in the middle of the NACME motif should be modified to protect from potential attack by cellular esterases. The nitrofuran group may yield a toxic metabolite in vivo because a structurally similar carcinogen semicarbazide is metabolically generated from the banned drug nitrofurazone.[34] These points should be considered in modifying the structure of the NACME core. Interestingly, a mutation in His539 decreases the polymerase activity by 50%.[1] Given that the NACME derivatives appear to interfere with His539, we may be able to generate a dual inhibitor targeting both RNase H and polymerase functions of HIV-1 RT.

Methods

Enzymes. A DNA fragment encoding the HIV-1 RT was amplified from molecular clones with the following primers: for p66, 5′- TGGTTGTACTTTAGGATCCCCAATTAGTCC-3′, and 5′- TATTCCATCGGATCCCTACTATAGCTCTTTCCTGATTC-3′; for p51, 5′-TGGTTGTACTTTAGGATCCCCAATTAGTCC-3′, and 5′-AGCCCCATCGGATCCCTACTAGAAAGTCTCTGC-3′. The PCR products were digested with *Bam*HI and cloned into the *Bam*HI site of pQE-9 (QIAGEN GmbH, Hilden, Germany) to generate plasmids expressing p66 or p51 RT with a hexahistidine tag at the amino terminus. The *E. coli* strain BL21(DE3)pLysS (Promega, Madison, WI) was transformed with the plasmids, and protein expression was induced by treatment with 1 mM isopropyl β-D-thiogalactoside for 3 h. The basic procedures for purification of the hexahistidine-tagged p66 and p51 monomers of HIV-1 RT have been described.[35,36] For heterodimer purification, bacteria expressing p66 or p51 were mixed prior to purification. The AKTA prime step gradient system (GE Healthcare Bio-Sciences, Piscataway, NJ) was used with HiTrap HP columns (GE Healthcare) according to the manufacturer's protocol. The yields of purified proteins were estimated using a Protein assay kit (Bio-Rad, Hercules, CA.) with bovine serum albumin as a standard. All

preparations were >95% pure, as estimated by inspection of Coomassie blue-stained SDS-polyacrylamide gels. The concentration of HIV-1 RT was approximately 1×10^4 units/g, as determined by comparing polymerase activity with that of an RT standard (Worthington Biochemical Corporation, Lakewood, NJ). Murine leukemia virus RT used in this study was obtained from New England Biolabs (Beverly, MA) and Promega. The *E. coli* RNase H was purchased from Sigma (St. Louis, MO). Activities were tested according to the manufacturers' protocols.

Screening of RNase H Inhibitors. Chemical compounds were purchased from Enamine Co. Ltd. (Ukraine). The purity of compounds **1** and **2** analyzed in detail was >99% according to the manufacturer (Enamine Co. Ltd.). For the first and second rounds of screening, the oligo ribonucleotide 5′-GGUCUCUCUGGUAGACCAGA-3′, corresponding to nucleotides 455−475 of HXB2 with 6-carboxy-fluoroscein (FAM) conjugated at the 5′ end was annealed to the oligo deoxyribonucleotide 5′-TCTGGTCTAACCAGAGAGACC-3′ using a final concentration of 1 μM each in annealing buffer containing 100 mM NaCl. Enzyme reactions containing 100 ng RT and 0.1 μM substrate were preincubated at 37 °C, and reactions were initiated by adding reaction buffer to yield the following final concentrations of components: 45 μM annealed oligos, 10 mM Tris-HCl, pH 7.8, 15 mM KCl, 1 mM $MgCl_2$, 0.4 mM DTT, 0.01% v/v nonionic detergent IGEPAL (Sigma), and 0.2 mM EDTA. Alternatively, the reaction was set up on ice in the reaction buffer and the reaction initiated by shifting the temperature to 37 °C. Both assay protocols yielded essentially the same results. The reactions were stopped by adding 3 μL of loading buffer containing 50% formamide, 25% glycerol, 2.5 mM EDTA, and a nucleic acid stain SYBR Green (1:10000 dilution, Invitrogen, Tokyo, Japan). A 4 μL aliquot was subjected to 4% urea-containing 18% PAGE for 60 min at 100 V, and the products were visualized by Typhoon9400 imager. For the third screening, a previously described real-time monitoring assay was used with the following modifications.[21] For substrates, the following oligonucleotides were annealed at final concentrations of 40 and 1 μM, respectively, in annealing buffer: oligo ribonucleotide 5′-GAUCUGAGCCUGGGAGCU-3′ with FAM conjugated at the 5′ end, and oligodeoxyribonucleotide 5′-AGCTCCCAGGCTCAGATC-3′ with black hole quencher (BHQ) conjugated at the 3′ end. Enzyme reactions containing 100 ng RT, 4 μM oligoribonucleotide, and 0.1 μM oligodeoxyribonucleotide were carried out in a volume of 10 μL at 37 °C in reaction buffer for the indicated times. Fluorescence at 488 nm signal was monitored every 150 s using a Multimode Detector (Beckman Coulter, Miami, FL).

Replication Monitoring. To produce HIV-1, 293T cells were transfected with plasmids encoding the HIV-1 proviral DNA (pNL4−3) and culture supernatants containing viruses were collected at 48 h post-transfection. For HIV-1 infection, 1.5×10^4 primary peripheral blood mononuclear cells depleted for $CD8^+$ T cells (denoted as primary $CD4^+$ T cells in the text) by MACS CD8 microbeads (Miltenyi Biotec, Tokyo) or 2×10^3 NP2CD4CXCR4 cells were incubated at the room temperature for approximately 4 hours with HIV-1-containing culture supernatant having approximately 250 pg of the viral antigen p24. IL-2 and anti-CD3 antibody-stimulated primary $CD4^+$ T cells were passaged every 2−4 days, and the culture supernatants were collected when cells were passaged. For NP2CD4CXCR4 cells, culture supernatants were collected at 4 days postinfection. The culture supernatants were subjected to an ELISA assay to measure the p24 antigen, as an indicator of virus production, using a Retro TEK p24 antigen ELISA kit according to the manufacturer's protocol (Zepto Metrix, Buffalo, NY). The ELISA reactions were measured using a ELx808 microplate photometer (BIO-TEK, Winooski, VT).

Measuring Cytotoxicity. IL-2 and anti-CD3 antibody-stimulated primary $CD4^+$ T cells were plated at a density of 2.5×10^4 cells per well in 96-well plates and maintained in culture for 6−7 days in the various concentration of chemical compounds. The cell proliferation was evaluated by the 3-(4,5-dimethylthiazol-2-yl)-2,5-diphenyltetrazolium bromide (MTT) assay (CellTiter 96 AQueous; Promega) according to manufacturer's instructions. The OD_{490} was measured by an ELISA reader (BIO-TEK). Wells with culture medium only were measured as background signal. For cell lines, assays were performed with 1×10^3 cells per well. The 50% cytotoxicity concentration was defined as a drug concentration by which the OD_{490} value reached the 50% level of the no drug control. The maximum concentrations of compounds we tested was 50 μM.

Protein Structure Preparation. An X-ray structure of HIV-1 RT was downloaded from the Protein Data Bank (PDB code: 1RTD[23]). This structure contains a DNA template, primer, dTTP containing two Mg^{2+} ions, and two Mg^{2+} ions in the RNase H active site in addition to the p66 and p51 domains. For the docking simulations, the DNA template, primer, and dTTP were deleted, and hydrogen atoms were added using the PDB2PQR web service.[37,38] The resulting.pqr file was modified manually, and was converted into a mol2 file using babel3 2.2 (OpenEye Scientific Software, Inc.).

Molecular Docking. The three-dimensional structures of the ligands used in this study were generated from a SMILES string by OMEGA 2.2.1 (OpenEye Scientific Software, Inc.). The binding models for HIV-1 RNase H inhibitors were predicted using the docking program GOLD 3.2 (CCDC Software Ltd., Cambridge, UK). The binding site was initially defined as all residues of the target within 10 Å of the Mg^{2+} ion coordinated by Asp443, Asp498, and Asp549. ChemScore was chosen as a fitness function and the standard default settings were used in all calculations.[39] The Mg^{2+} ions were set to allow hexavalent coordination. Early termination was allowed for searching the ligand docking poses. In early termination mode, calculation is stopped when the root-mean-square deviation (rmsd) on heavy atoms of the ligand among top three high scoring docking poses are within 15 Å of the target. An additional docking simulation was executed using Glide 4.0 (Schrodinger Inc.) with equivalent calculation conditions.

Acknowledgment. We thank Dr. Beutler's and Dr. Pommier's laboratory groups in the National Cancer Institute for measuring the IC_{50}s of compounds **1** and **2** against human RNase H1 and HIV-1 RT and against HIV-1 IN, respectively. We appreciate Dr. Sato's group for sharing purified CRF01 A_E RT (National Institute of Infectious Diseases, Tokyo). This work was supported by the Japan Health Science Foundation, the Japanese Ministry of Health, Labor, and Welfare (H18-AIDS-W-003) and the Japanese Ministry of Education, Culture, Sports, Science, and Technology (18689014 and 18659136).

Supporting Information Available: Alignment of reverse transcriptase amino acid sequences of the clade B B.FR.x.pNL43, clade C Indie-C1, and 93JP-NH1, a representative of CRF01_AE. This material is available free of charge via the Internet at http://pubs.acs.org.

References

(1) Nikolenko, G. N.; Svarovskaia, E. S.; Delviks, K. A.; Pathak, V. K. Antiretroviral drug resistance mutations in human immunodeficiency virus type 1 reverse transcriptase increase template-switching frequency. *J. Virol.* **2004**, *78*, 8761–8770.

(2) Nikolenko, G. N.; Palmer, S.; Maldarelli, F.; Mellors, J. W.; Coffin, J. M.; Pathak, V. K. Mechanism for nucleoside analog-mediated abrogation of HIV-1 replication: balance between RNase H activity and nucleotide excision. *Proc. Natl. Acad. Sci. U.S.A* **2005**, *102*, 2093−2098. Epub 2005 Jan 2031.

(3) Luo, G. X.; Taylor, J. Template switching by reverse transcriptase during DNA synthesis. *J. Virol.* **1990**, *64*, 4321–4328.

(4) Peliska, J. A.; Benkovic, S. J. Mechanism of DNA strand transfer reactions catalyzed by HIV-1 reverse transcriptase. *Science* **1992**, *258*, 1112–1118.

(5) DeStefano, J. J.; Mallaber, L. M.; Rodriguez-Rodriguez, L.; Fay, P. J.; Bambara, R. A. Requirements for strand transfer between internal regions of heteropolymer templates by human immunodeficiency virus reverse transcriptase. *J. Virol.* **1992**, *66*, 6370–6378.

(6) DeStefano, J. J.; Roberts, B.; Shriner, D. The mechanism of retroviral recombination: the role of sequences proximal to the point of strand transfer. *Arch. Virol.* **1997**, *142*, 1797–1812.

(7) DeStefano, J. J.; Bambara, R. A.; Fay, P. J. The mechanism of human immunodeficiency virus reverse transcriptase-catalyzed strand transfer from internal regions of heteropolymeric RNA templates. *J. Biol. Chem.* **1994**, *269*, 161–168.
(8) Klumpp, K.; Mirzadegan, T. Recent progress in the design of small molecule inhibitors of HIV RNase H. *Curr. Pharm. Des.* **2006**, *12*, 1909–1922.
(9) Borkow, G.; Fletcher, R. S.; Barnard, J.; Arion, D.; Motakis, D.; Dmitrienko, G. I.; Parniak, M. A. Inhibition of the ribonuclease H and DNA polymerase activities of HIV-1 reverse transcriptase by *N*-(4-*tert*-butylbenzoyl)-2-hydroxy-1-naphthaldehyde hydrazone. *Biochemistry* **1997**, *36*, 3179–3185.
(10) Sluis-Cremer, N.; Arion, D.; Parniak, M. A. Destabilization of the HIV-1 reverse transcriptase dimer upon interaction with *N*-acyl hydrazone inhibitors. *Mol. Pharmacol.* **2002**, *62*, 398–405.
(11) Marchand, C.; Beutler, J. A.; Wamiru, A.; Budihas, S.; Mollmann, U.; Heinisch, L.; Mellors, J. W.; Le Grice, S. F.; Pommier, Y. Madurahydroxylactone derivatives as dual inhibitors of human immunodeficiency virus type 1 integrase and RNase H. *Antimicrob. Agents Chemother.* **2008**, *52*, 361−364. Epub 2007 Oct 2029.
(12) Tramontano, E.; Esposito, F.; Badas, R.; Di Santo, R.; Costi, R.; La Colla, P. 6-[1-(4-Fluorophenyl)methyl-1*H*-pyrrol-2-yl)]-2,4-dioxo-5-hexenoic acid ethyl ester a novel diketo acid derivative which selectively inhibits the HIV-1 viral replication in cell culture and the ribonuclease H activity in vitro. *Antivir. Res.* **2005**, *65*, 117–124.
(13) Tarrago-Litvak, L.; Andreola, M. L.; Fournier, M.; Nevinsky, G. A.; Parissi, V.; de Soultrait, V. R.; Litvak, S. Inhibitors of HIV-1 reverse transcriptase and integrase: classical and emerging therapeutical approaches. *Curr. Pharm. Des.* **2002**, *8*, 595–614.
(14) Moelling, K.; Schulze, T.; Diringer, H. Inhibition of human immunodeficiency virus type 1 RNase H by sulfated polyanions. *J. Virol.* **1989**, *63*, 5489–5491.
(15) Loya, S.; Hizi, A. The interaction of illimaquinone, a selective inhibitor of the RNase H activity, with the reverse transcriptases of human immunodeficiency and murine leukemia retroviruses. *J. Biol. Chem.* **1993**, *268*, 9323–9328.
(16) Tan, C. K.; Civil, R.; Mian, A. M.; So, A. G.; Downey, K. M. Inhibition of the RNase H activity of HIV reverse transcriptase by azidothymidylate. *Biochemistry* **1991**, *30*, 4831–4835.
(17) Davis, W. R.; Tomsho, J.; Nikam, S.; Cook, E. M.; Somand, D.; Peliska, J. A. Inhibition of HIV-1 reverse transcriptase-catalyzed DNA strand transfer reactions by 4-chlorophenylhydrazone of mesoxalic acid. *Biochemistry* **2000**, *39*, 14279–14291.
(18) Klumpp, K.; Hang, J. Q.; Rajendran, S.; Yang, Y.; Derosier, A.; Wong Kai In, P.; Overton, H.; Parkes, K. E.; Cammack, N.; Martin, J. A. Two-metal ion mechanism of RNA cleavage by HIV RNase H and mechanism-based design of selective HIV RNase H inhibitors. *Nucleic Acids Res.* **2003**, *31*, 6852–6859.
(19) Shaw-Reid, C. A.; Munshi, V.; Graham, P.; Wolfe, A.; Witmer, M.; Danzeisen, R.; Olsen, D. B.; Carroll, S. S.; Embrey, M.; Wai, J. S.; Miller, M. D.; Cole, J. L.; Hazuda, D. J. Inhibition of HIV-1 ribonuclease H by a novel diketo acid, 4-[5-(benzoylamino)thien-2-yl]-2,4-dioxobutanoic acid. *J. Biol. Chem.* **2003**, *278*, 2777−2780. Epub 2002 Dec 2711.
(20) Himmel, D. M.; Sarafianos, S. G.; Dharmasena, S.; Hossain, M. M.; McCoy-Simandle, K.; Ilina, T.; Clark, A. D., Jr.; Knight, J. L.; Julias, J. G.; Clark, P. K.; Krogh-Jespersen, K.; Levy, R. M.; Hughes, S. H.; Parniak, M. A.; Arnold, E. HIV-1 reverse transcriptase structure with RNase H inhibitor dihydroxy benzoyl naphthyl hydrazone bound at a novel site. *ACS Chem. Biol.* **2006**, *1*, 702–712.
(21) Parniak, M. A.; Min, K. L.; Budihas, S. R.; Le Grice, S. F.; Beutler, J. A. A fluorescence-based high-throughput screening assay for inhibitors of human immunodeficiency virus-1 reverse transcriptase-associated ribonuclease H activity. *Anal. Biochem.* **2003**, *322*, 33–39.
(22) Chan, K. C.; Budihas, S. R.; Le Grice, S. F.; Parniak, M. A.; Crouch, R. J.; Gaidamakov, S. A.; Isaaq, H. J.; Wamiru, A.; McMahon, J. B.; Beutler, J. A. A capillary electrophoretic assay for ribonuclease H activity. *Anal. Biochem.* **2004**, *331*, 296–302.
(23) Huang, H.; Chopra, R.; Verdine, G. L.; Harrison, S. C. Structure of a covalently trapped catalytic complex of HIV-1 reverse transcriptase: implications for drug resistance. *Science* **1998**, *282*, 1669–1675.
(24) Katayanagi, K.; Okumura, M.; Morikawa, K. Crystal structure of *Escherichia coli* RNase HI in complex with Mg^{2+} at 2.8 A resolution: proof for a single Mg(2+)-binding site. *Proteins* **1993**, *17*, 337–346.
(25) Nowotny, M.; Gaidamakov, S. A.; Ghirlando, R.; Cerritelli, S. M.; Crouch, R. J.; Yang, W. Structure of human RNase H1 complexed with an RNA/DNA hybrid: insight into HIV reverse transcription. *Mol. Cell* **2007**, *28*, 264–276.
(26) Eldridge, M. D.; Murray, C. W.; Auton, T. R.; Paolini, G. V.; Mee, R. P. Empirical scoring functions: I. The development of a fast empirical scoring function to estimate the binding affinity of ligands in receptor complexes. *J. Comput.-Aided Mol. Des.* **1997**, *11* (5), 425–45.
(27) Smith, J. S.; Roth, M. J. Purification and characterization of an active human immunodeficiency virus type 1 RNase H domain. *J. Virol.* **1993**, *67*, 4037–4049.
(28) Sarafianos, S. G.; Das, K.; Tantillo, C.; Clark, A. D. Jr.; Ding, J.; Whitcomb, J. M.; Boyer, P. L.; Hughes, S. H.; Arnold, E. Crystal structure of HIV-1 reverse transcriptase in complex with a polypurine tract RNA:DNA. *EMBO J.* **2001**, *20*, 1449–1461.
(29) Schatz, O.; Cromme, F. V.; Gruninger-Leitch, F.; Le Grice, S. F. Point mutations in conserved amino acid residues within the C-terminal domain of HIV-1 reverse transcriptase specifically repress RNase H function. *FEBS Lett.* **1989**, *257*, 311–314.
(30) Nikolenko, G. N.; Delviks-Frankenberry, K. A.; Palmer, S.; Maldarelli, F.; Fivash, M. J.; Coffin, J. M.; Pathak, V. K. Mutations in the connection domain of HIV-1 reverse transcriptase increase 3′-azido-3′-deoxythymidine resistance. *Proc. Natl. Acad. Sci. U.S.A.* **2007**, *104*, 317−322. Epub 2006 Dec 2019.
(31) Brehm, J. H.; Koontz, D.; Meteer, J. D.; Pathak, V.; Sluis-Cremer, N.; Mellors, J. W. Selection of mutations in the connection and RNase H domains of human immunodeficiency virus type 1 reverse transcriptase that increase resistance to 3′-azido-3′-dideoxythymidine. *J. Virol.* **2007**, *81*, 7852−7859. Epub 2007 May 7816.
(32) Delviks-Frankenberry, K. A.; Nikolenko, G. N.; Barr, R.; Pathak, V. K. Mutations in human immunodeficiency virus type 1 RNase H primer grip enhance 3′-azido-3′-deoxythymidine resistance. *J. Virol.* **2007**, *81*, 6837−6845. Epub 2007 Apr 6811.
(33) Radzio, J.; Sluis-Cremer, N. Efavirenz accelerates HIV-1 reverse transcriptase ribonuclease H cleavage, leading to diminished zidovudine excision. *Mol. Pharmacol.* **2008**, *73*, 601−606. Epub 2007 Nov 2016.
(34) Hirakawa, K.; Midorikawa, K.; Oikawa, S.; Kawanishi, S. Carcinogenic semicarbazide induces sequence-specific DNA damage through the generation of reactive oxygen species and the derived organic radicals. *Mutat. Res.* **2003**, *536*, 91–101.
(35) Kim, B.; Hathaway, T. R.; Loeb, L. A. Human immunodeficiency virus reverse transcriptase. Functional mutants obtained by random mutagenesis coupled with genetic selection in *Escherichia coli*. *J. Biol. Chem.* **1996**, *271*, 4872–4878.
(36) Kim, B.; Hathaway, T. R.; Loeb, L. A. Fidelity of mutant HIV-1 reverse transcriptases: interaction with the single-stranded template influences the accuracy of DNA synthesis. *Biochemistry* **1998**, *37*, 5831–5839.
(37) Dolinsky, T. J.; Nielsen, J. E.; McCammon, J. A.; Baker, N. A. PDB2PQR: an automated pipeline for the setup of Poisson−Boltzmann electrostatics calculations. *Nucleic Acids Res.* **2004**, *32*, W665–W667.
(38) Dolinsky, T. J.; Czodrowski, P.; Li, H.; Nielsen, J. E.; Jensen, J. H.; Klebe, G.; Baker, N. A. PDB2PQR: expanding and upgrading automated preparation of biomolecular structures for molecular simulations. *Nucleic Acids Res.* **2007**, *35*, W522−W525. Epub 2007 May 2008.
(39) Verdonk, M. L.; Cole, J. C.; Hartshorn, M. J.; Murray, C. W.; Taylor, R. D. Improved protein−ligand docking using GOLD. *Proteins* **2003**, *52* (4), 609–623.

JM801071M